Effect of electronic-ballast fluorescent lighting on wireless infrared links

R.Narasimhan
M.D.Audeh
J.M.Kahn

Indexing terms: Wireless infrared links, Electronic ballast, Fluorescent lighting

Abstract: Fluorescent lamps driven by electronic ballasts emit an infrared (IR) signal that is periodically modulated at rates of tens of kilohertz, and which can severely impair the performance of IR wireless links. The impact of fluorescent interference can potentially be reduced by highpass electrical filtering, but such filtering induces intersymbol interference (ISI). The authors present expressions for the bit error rate (BER) of systems using on-off keying (OOK) and pulse-position modulation (PPM) in the presence of both a deterministic interfering signal and ISI. They have measured the interference waveforms from lamps driven by 22 and 45kHz ballasts, and have used the measured waveforms to evaluate the performance of IR links using OOK and 2, 4, 8 and 16PPM at bit rates of 1, 10, and 100Mbit/s. When the fluorescent interference is normalised to the signal power required in the absence of this interference, the penalties incurred by OOK are found to be essentially independent of bit rate. At 1Mbit/s, PPM suffers approximately the same penalties as OOK, but as the bit rate is increased, the degradation of PPM becomes progressively much smaller. In the absence of measures to prevent ISI, first-order highpass filtering is not effective in improving the performance of OOK, but can substantially improve PPM link performance at bit rates of 10 and 100Mbit/s.

1 Introduction

Infrared (IR) systems represent a feasible alternative to radio systems [1–3] for many applications of indoor wireless communication. The IR spectrum is unregulated and provides a large capacity. Furthermore, since the square-law photodetector used in a direct-detection system is many times larger than the IR wavelength, no multipath fading occurs [4]. However, distortion due to multipath propagation is present.

Many IR systems operate in the presence of steady, high-intensity background radiation, which induces nearly white shot noise. The background-induced shot noise typically has a power from 10^2 to 10^4 times greater than the signal shot noise [3]. Thus, the signal shot noise can be neglected, and the ambient-induced shot noise can be considered Gaussian, due to its high intensity, and additive, since there is no effective mixing of signal and noise. In situations where the steady background illumination is sufficienfly weak, the dominant source of noise is the receiver thermal noise, which can be modelled as additive and Gaussian.

In contrast to the steady background radiation mentioned above, fluorescent lighting induces interference that is nearly deterministic and periodic, since the fluorescent light flickers at a constant rate determined by the lamp drive frequency. At present, most lamps are driven at the power-line frequency of 50 or 60Hz, and they induce interference at harmonics of the power-line frequency, up to ~50kHz [5, 6]. While this interference is potentially detrimental to IR links, it can usually be easily eliminated by careful choice of modulation scheme, and through electrical highpass filtering, as shown in a recent study by Moreira *et al.* [7]. Recent years have seen the introduction of 'electronic ballasts', which use switching transistors to modulate the power at a high frequency (typically tens of kilohertz), resulting in a ballast of improved efficiency and reduced size. As shown in this paper and elsewhere [6], lamps driven by electronic ballasts induce interference at harmonics of the ballast modulation frequency, extending up to ~1MHz. Owing to the much wider frequency range of their interference, electronic ballasts represent a much more serious impairment than their conventional counterparts. Moreira *et al.* have shown that even when optimised highpass electrical filtering is used, interference from electronic-ballast-driven lamps can cause sizeable power penalties.

2 Characterisation of emission from electronic-ballast fluorescent lamps

Fig. 1 shows the time-averaged optical emission spectrum of a typical fluorescent lamp (cool white phosphor, 40W, 1.5in diam., 8ft long). At wavelengths shorter than ~700nm, light emitted along the tube's entire length has the same spectrum. At longer wavelengths, which are of interest for IR communication systems, spectral lines from mercury are emitted along

IEE Proceedings online no. 19960877

Paper first received 11th June 1996 and in final revised form 26th September 1996

R. Narasimhan is with the Department of Electrical Engineering, Stanford University, Stanford, CA 94305, USA

M.D. Auden is with Telesis Technologies Lab, 5000 Executive Parkway, Suite 333, San Ramon, CA 94583, USA

J.M. Kahn is with the Department of Electrical Engineering and Computer Sciences, University of California, Berkeley, CA 94720, USA

the tube's entire length, but those from argon are emitted primarily from regions lying within 10cm of either end of the tube.

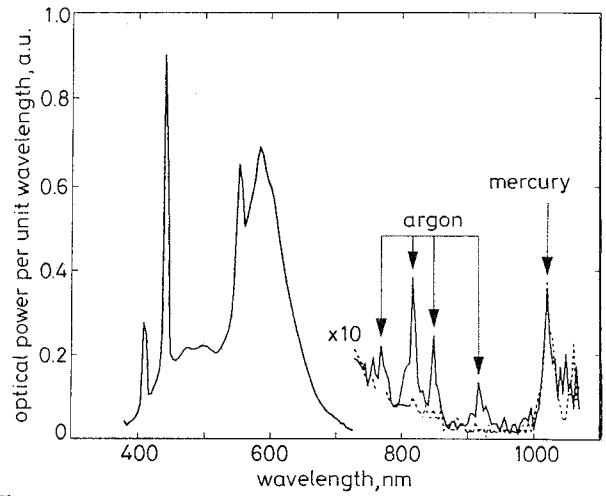

Fig. 1 *Optical spectrum of emission from a typical fluorescent lamp*
5nm resolution BW
——— end of tube
– – – – centre of tube

We measured the electrical interference from lamps driven by electronic ballasts at frequencies of 22kHz (Cool white phosphor, 40W, 1.4in diam., 4ft long, driven by fixture with integral ballast. Magnatek Triad model B240R120.) and 45kHz (15W lamp with integral ballast, designed to screw into standard incandescent lamp sockets. Philips model SLS15). In these measurements, we used a receiver using a silicon *pin* photodiode covered by an optical bandpass filter with a centre wavelength of 815nm and a bandwidth of 30nm. (Examination of Fig. 1 suggests that this receiver would mainly detect the lamp's argon emission; we note that very similar electrical interference waveforms were recorded when no optical bandpass filter was used). The receiver preamplifier had a 3dB electrical bandwidth extending from 1.5kHz to 23.4MHz. In a real communication system, the receiver may detect emission from several fluorescent lamps driven by one or more ballasts. Unlike the case of lamps driven by the power line, emissions from lamps driven by different electronic ballasts are generally not synchronised. Hence, for a given time-averaged fluorescent-induced photocurrent (corresponding to a given useful illumination level), the waveform from one or more lamps driven by a single ballast will generally have the greatest possible amplitude excursion and slope, and will thus represent the worst case. For this reason, we have measured the interference from lamps driven by a single ballast.

Table 1 compares the ratios of the photocurrent excursions (from the mean photocurrent) to the mean photocurrent for the waveforms emitted by the 22 and 45kHz lamps. For a given mean photocurrent (corresponding to a given useful lighting level), the 45kHz waveform exhibits somewhat greater excursions from the mean value than does the 22kHz waveform. The electrical power spectrum of the 22kHz lamp emission is shown in Fig. 2; the spectrum from the 45kHz lamp is qualitatively similar to this. In the spectrum in Fig. 2, the first few even harmonics of 22kHz are markedly stronger than the first few odd harmonics [6]. Harmonics of 22kHz are detectable above the receiver noise floor at frequencies up to ~1MHz.

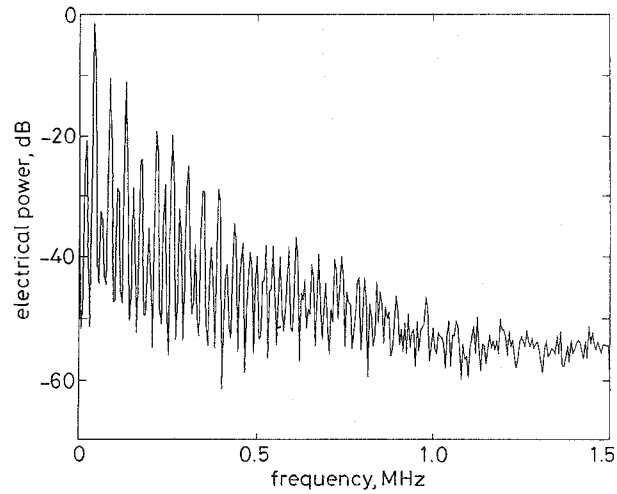

Fig. 2 *Electrical spectrum of fluorescent light emission from lamp driven by a 22kHz electonic ballast*
Reference level arbitrarily set to 0dB

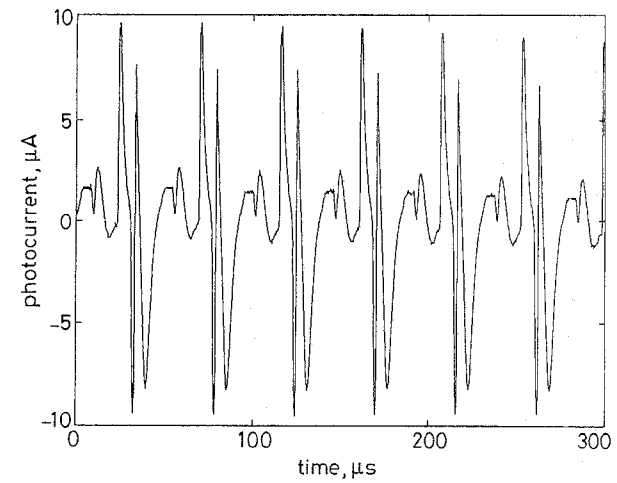

Fig. 3 *Photocurrent waveform from a lamp driven by a 22kHz electronic ballast*
DC component of the waveform has beeen removed

We used a digitising oscilloscope to sample the fluorescent emission waveforms; the sampling rate of 5MHz is well above the Nyquist rate. Fig. 3 displays a few periods of the waveform emitted by the 22kHz lamp; the waveform emitted by the 45kHz lamp is qualitatively similar to this one. The waveform in Fig. 3 displays abrupt transitions, some of which have rise times as small as 2μs. It is worth noting that power spectra from 22 and 45kHz lamps also exhibit harmon-

Table 1: Comparison of ratios of photocurrent excursions to mean photocurrents for lamps driven by 22 and 45kHz ballasts

Ballast frequency (kHz)	Maximum–Mean / Mean	Mean–Minimum / Mean	Maximum–Minimum / Mean
22	0.582	0.576	1.158
45	1.125	0.628	1.753

ics of the power-line frequency (60Hz), and that the waveforms exhibit corresponding slow amplitude variations of the order of 7%. While these effects are not evident in Figs. 2 and 3, they are included in the performance evaluations presented in Section 4.

3 Performance analysis of links using OOK and L-PPM

In this Section, we present expressions for the BER of IR links using OOK and L-PPM. We begin by treating the case where fluorescent-light interference is present but no highpass filtering is used. Owing to the lowpass characteristic of the fluorescent-light interference, we would like to use a highpass filter to attenuate it, but this will induce intersymbol interference (ISI). We assume perfect synchronisation of transmitter and receiver, and neglect multipath distortion. Although the latter assumption is valld for all bit rates of interest for directed, line-of-sight links, the assumption is not valid for bit rates above ~10Mbit/s in non-directed links [4].

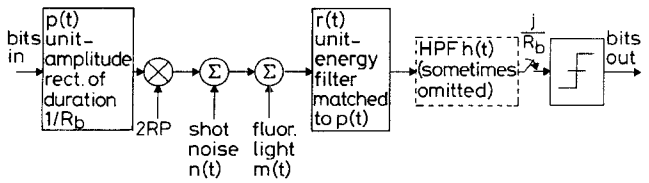

Fig. 4 *Block diagram of OOK system*

The block diagram of the OOK system under consideration is shown in Fig. 4. The input bits, at rate R_b, are assumed to be independent, identically distributed (IID) and uniform on {0, 1}. These bits are passed through a transmitter filter whose impulse response $p(t)$ is a unit-amplitude rectangle of duration equal to $1/R_b$. The result is scaled by the peak detected signal photocurrent $2RP$, where P is the average received optical signal power and R is the photodetector responsivity. The additive shot noise $n(t)$ is independent of the received signal, and is modelled as zero-mean, Gaussian, and white, with double-sided power spectral density (PSD) N_0. The detected fluorescent-light photocurrent waveform $m(t)$ is assumed to have zero mean value and a maximum absolute excursion of RP_f from the mean value. The receiver uses a unit-energy filter $r(t)$ matched to $p(t)$. In some cases, the signal is passed through a highpass filter with impulse response $h(t)$. The resulting signal is sampled at rate R_b and passed to a slicer, which yields the output bits. The slicer threshold is set at $RP/\sqrt{R_b}$, midway between the nominal '0' and '1' levels. We note that when fluorescent lighting and highpass filtering are ignored, this represents a maximum-likelihood (ML) receiver. Our choice of threshold level and assumption that $m(t)$ has zero mean are equivalent to the practical case of an AC-coupled receiver whose slicer threshold is set to 0V.

Fig. 5 shows the block diagram of the L-PPM system. Input bits, at rate R_b, enter a PPM encoder, producing L-PPM symbols at rate $R_b/\log_2 L$. Each symbol contains a single sample of unit amplitude, and L–1 samples of zero amplitude. The PPM symbols are converted to a serial sequence of chips at rate $LR_b/\log_2 L$, and passed to a transmitter filter whose impulse response $p(t)$ is a unit-amplitude rectangular pulse of duration $\log_2 L/LR_b$. The chips are scaled by the peak detected signal photocurrent LRP, and shot noise $n(t)$ and fluorescent-light interference $m(t)$ are added. The receiver employs a unit-energy filter $r(t)$ matched to $p(t)$, which is followed, in some cases, by a highpass filter $h(t)$. The filtered signal is sampled at rate $LR_b/\log_2 L$ and passed to a comparator that determines which sample in each L-length block has the largest value, thus yielding the output bit sequence. We note that when fluorescent lighting and highpass filtering are ignored, this represents a ML receiver.

3.1 Effect of fluorescent lighting without highpass filtering

Let m_j denote the samples of the fluorescent-light waveform at the slicer:

$$m_j = m(t) \otimes r(t)\Big|_{t=\frac{j}{R_b}} \tag{1}$$

where the symbol $\otimes$ denotes convolution. We consider a transmission whose length is M bits, and average the BER obtained for each of the M values of m_j and for each of the possible transmitted bits '0' and '1'. The average BER of the OOK system is given by:

$$P[\text{bit error}] = \frac{1}{2M}\sum_{j=1}^{M}\left[Q\left(\frac{\frac{RP}{\sqrt{R_b}}+m_j}{\sqrt{N_0}}\right)+Q\left(\frac{\frac{RP}{\sqrt{R_b}}-m_j}{\sqrt{N_0}}\right)\right] \tag{2}$$

where

$$Q(x) = \frac{1}{\sqrt{2\pi}}\int_x^\infty e^{-\frac{y^2}{2}}dy$$

The probability of bit error for the PPM system is computed using the union (upper) bound, which is extremely accurate at below the BERs of interest here (10^{-9}). The chip-rate fluorescent-light samples m_j are obtained using eqn. 1, with the sampling times replaced by $t = j\log_2 L/LR_b$. Assume that the transmission spans M/L symbols. Averaging over these M/L different symbol periods, each with its own values of m_j with L possible transmitted symbols, and with L–1 possible incorrectly detected symbols, we obtain the union bound for the probability of bit error:

$$P[\text{bit error}] \le \frac{1}{M}\cdot\frac{L/2}{L-1}\sum_{n=0}^{\frac{M}{L}-1}\sum_{j=0}^{L-1}\sum_{i=0}^{L-1} \times Q\left(\frac{\frac{RP\sqrt{L\log_2 L}}{\sqrt{R_b}}+m_{nL+j}-m_{nL+i}}{\sqrt{2N_0}}\right) \tag{3}$$

The factor $(L/2)/(L-1)$ represents the average number of bit errors per symbol error.

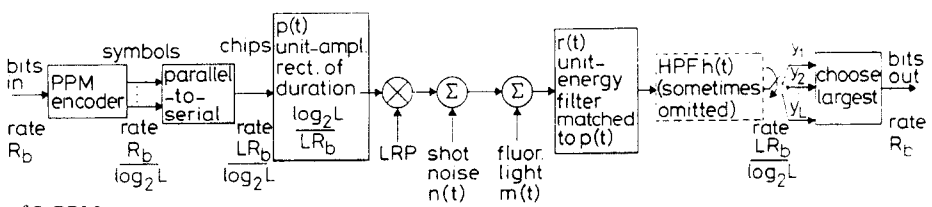

Fig. 5 *Block diagram of L-PPM system*

3.2 Effect of highpass filtering without fluorescent lighting

We analysed the BER in the presence of the ISI caused by highpass filtering, ignoring the effect of the fluorescent-light interference. The basic analysis technique is as follows: the highpass filter is introduced and the discrete-time equivalent impulse response of the cascaded transmitter filter, receiver filter, and highpass filter is calculated. The resulting system has an infinite-duration impulse response, but because it decays rapidly to zero with time, it can be truncated without significant loss of accuracy. All possible symbol sequences with a length equal to the truncated impulse response are enumerated. The BER is calculated for each sequence and then averaged over all possible sequences to obtain the average BER. This technique has been used previously to compute ISI penalties in systems using OOK [8] and L-PPM [9].

Assuming OOK is used, the discrete-time impulse response, truncated to have a duration of J bit periods, is:

$$c_j = \begin{cases} p(t) \otimes r(t) \otimes h(t)\Big|_{t=\frac{j}{R_b}}, & 0 \le j \le J-1 \\ 0, & \text{otherwise} \end{cases} \tag{4}$$

with the normalisation $\Sigma_j c_j = 1$. Let $\mathbf{a}_j$ denote a transmitted bit sequence of length J and suppose that the correct sampling point occurs at $j = 0$. The average probability of bit error for the OOK system is given by:

$$P[\text{bit error}] = \frac{1}{2^J} \sum_{\mathbf{a}_j \in \{0,1\}^J} Q\left(\frac{RP\left|2(\mathbf{a}_j \otimes c_j)\Big|_{j=0} - 1\right|}{\sqrt{R_b N_0}} \right) \tag{5}$$

In the case of L-PPM, the truncated discrete-time impulse response is assumed to span K symbols, so it is given by an expression like eqn. 4, but with the sampling times replaced by $t = j\log_2 L/LR_b$, and with J replaced by LK. Let $\mathbf{b}_j$ denote a transmitted chip sequence of length LK chips. The union bound for the average probability of bit error for the PPM system is given by:

$$P[\text{bit error}] \le \frac{1}{L^K} \cdot \frac{L/2}{L-1} \sum_{\mathbf{b}_j} \sum_{\substack{i=0 \\ i \ne k}}^{L-1} \times Q\left(\frac{RP\sqrt{L\log_2 L}}{\sqrt{2}R_b N_0} [(\mathbf{b}_j \otimes c_j)\Big|_k - (\mathbf{b}_j \otimes c_j)\Big|_i] \right) \tag{6}$$

where, in the symbol being detected, a '1' chip was transmitted in position k.

3.3 Effect of fluorescent lighting with highpass filtering

Considering OOK, again let c_j have a duration of J bit periods. The fluorescent light samples are given by:

$$m_j = m(t) \otimes r(t) \otimes h(t)\Big|_{t=\frac{j}{R_b}} \tag{7}$$

Let $\mathbf{a}_j$ denote a transmitted bit sequence of length J. Assuming that the transmission spans M bits, the average probability of bit error for OOK is given by:

$$P[\text{bit error}] = \frac{1}{2M \cdot 2^J} \sum_{k=1}^{M} \sum_{\mathbf{a}_j \in \{0,1\}^J} \left[Q\left(\frac{\frac{RP}{\sqrt{R_b}}[2(\mathbf{a}_j \otimes c_j)\big|_{j=0} - 1] + m_k}{\sqrt{N_0}} \right) + Q\left(\frac{\frac{RP}{\sqrt{R_b}}[1 - 2(\mathbf{a}_j \otimes c_j)\big|_{j=0} - 1] - m_k}{\sqrt{N_0}} \right) \right] \tag{8}$$

In the case of a PPM system, again assume that the truncated impulse response c_j spans K symbols. Let $\mathbf{b}_j$ denote a transmitted chip sequence of length LK chips. The chip-rate fluorescent-light samples m_j are obtained using eqn. 7, with the sampling times replaced by $t = j\log_2 L/LR_b$. Assume that the transmission spans M/L symbols. The union bound for the probability of bit error is given by:

$$P[\text{bit error}] \le \frac{1}{L^K} \cdot \frac{L}{M} \cdot \frac{L/2}{L-1} \sum_{n=0}^{\frac{M}{L}-1} \sum_{\mathbf{b}_j} \sum_{\substack{i=0 \\ i \ne k}}^{L-1} \times Q\left(\frac{\frac{RP\sqrt{L\log_2 L}}{\sqrt{R_b}}[(\mathbf{b}_j \otimes c_j)\big|_{nL+k} - (\mathbf{b}_j \otimes c_j)\big|_{nL+i}] + m_{nL+k} - m_{nL+i}}{\sqrt{2N_0}} \right) \tag{9}$$

where, in the symbol being detected, a '1' chip was transmitted in position k.

4 Performance evaluation using measured fluorescent light emissions

We have used the fluorescent-light waveforms presented in Section 2, in conjunction with the BER expressions presented in Section 3 to numerically predict the performance of links using OOK and 2, 4, 8, and 16PPM at bit rates of 1, 10 and 100Mbit/s. As previously stated, we neglect the impact of multipath distortion, an assumption that breaks down at bit rates of ~10Mbit/s and higher on nondirected links.

We used fluorescent-light waveform records of 18ms duration. This represents hundreds of periods of the large amplitude oscillations caused by the 22 or 45kHz drive signal, and represents more than one period of the small amplitude variations induced by the 60Hz power-line signal (see Section 2). The mean values were subtracted from the fluorescent-light waveforms and the waveforms were interpolated to a sample rate of 800MHz prior to filtering by the receiver matched filter and highpass filter. The first-order highpass filter was implemented using the bilinear transformation. The continuous-time highpass filter has asymptotic unit gain at high frequencies, which requires that the discrete-time highpass filter with transfer function $H(z)$ satisfies $H(-1) = 1$.

When fluorescent-light interference and/or highpass filtering are introduced, the achievement of a desired BER will require an increased signal-to-Gaussian noise ratio (SNR) or, equivalently, a higher average received optical power. We define the SNR as SNR = $(RP)^2/N_0R_b$. This SNR is not equivalent to the usual E_b/N_0; instead, it is defined such that a 1dB change in average optical power corresponds to a 2dB change in SNR.

We parameterise the strength of the fluorescent interference as follows: first, we define $P_0 = 5.997\sqrt{\{R_bN_0\}}/R$, which is the average received optical signal power required to achieve 10^{-9} BER using OOK (or 2 PPM) in the absence of the fluorescent interference and highpass filtering. We then define P_f to be the peak absolute excursion of the fluorescent-light optical power waveform with respect to its mean value, so that RP_f is the maximum absolute excursion of the zero-mean fluorescent photocurrent waveform $m(t)$ from its mean

value. We note that P_f is proportional to the average received optical power due to fluorescent lighting. For the 22 and 45kHz ballasts considered here, the constants of proportionality are 0.582 and 1.125, based on the data in Table 1. The strength of the fluorescent interference is parameterised in terms of the ratio P_f/P_0. We note that since P_0 is proportional to the square root of the bit rate R_b, a given value of P_f/P_0 corresponds to different values of P_f at different bit rates. We quantify the fluorescent interference in terms of the ratio P_f/P_0. This choice is convenient because, at the high bit rates considered here, in the absence of highpass filtering, OOK suffers an SNR degradation that essentially only depends on P_f/P_0, and is nearly independent of the bit rate (see the following Section).

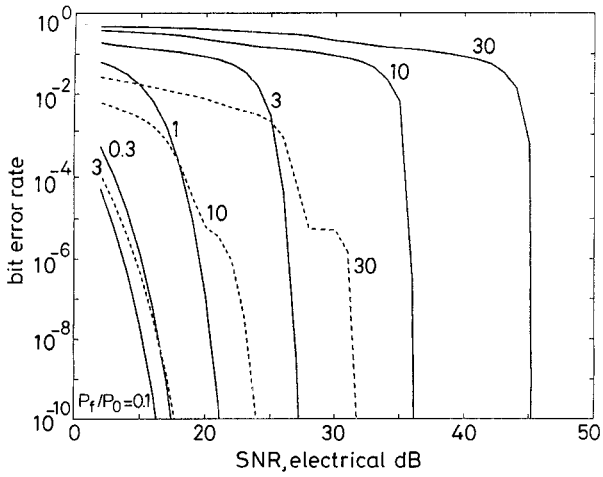

Fig. 6 *BER curves for various ratios of P_f/P_0 for OOK and 2 PPM at 10Mbit/s*
The fluorescent lamp is driven by a 22kHz ballast, and no highpass filter is employed
P_f maximum absolute excursion (with respect to the mean) of the received fluorescent optical power waveform
P_0 average optical power required to achieve 10^{-9} BER with OOK, in the absence of fluorescent lighting
——— OOK
- - - - 2 PPM

Fig. 6 illustrates an example of the BER against SNR performance of links subject to fluorescent-light interference without highpass filtering, computed using the expressions given in Section 3.1. This figure considers a 10Mbit/s link subject to interference from a 22kHz lamp. It compares the performance of OOK and 2 PPM, whose performance is theoretically identical in the absence of fluorescent-light interference. In Fig. 6, we see that for both OOK and 2 PPM, as P_f/P_0 increases, there is an increase in the SNR required to achieve 10^{-9} BER. We note, however, that OOK is degraded much more rapidly than 2 PPM. This can be understood by observing that the OOK slicer is sensitive to the actual values of the fluorescent-light samples, whereas the 2 PPM 'choose largest' detector is affected only by the differences between pairs of successive samples. (Of course, for a fixed bit rate, the 2 PPM detector uses a sample rate twice as high as the OOK detector.)

In Fig. 7 we examine the SNR requirements of various modulation schemes at a bit rate of 10Mbit/s, without highpass filtering, subject to interference from 22 and 45kHz lamps. To obtain these SNR requirements, we have computed BER against SNR curves at various values of P_f/P_0 (like those of Fig. 6), determined the SNR at which each curve crosses 10^{-9} BER, and then performed a spline fit to the resulting data of SNR requirement against P_f/P_0. At small values of P_f/P_0, the performance of all modulation schemes is nearly ideal, and higher-order PPM is seen to yield large decreases in the SNR (or power) requirements [2]. As the ratio P_f/P_0 increases, OOK is seen to degrade much more rapidly than the various PPM schemes, for reasons analogous to those given in the previous paragraph.

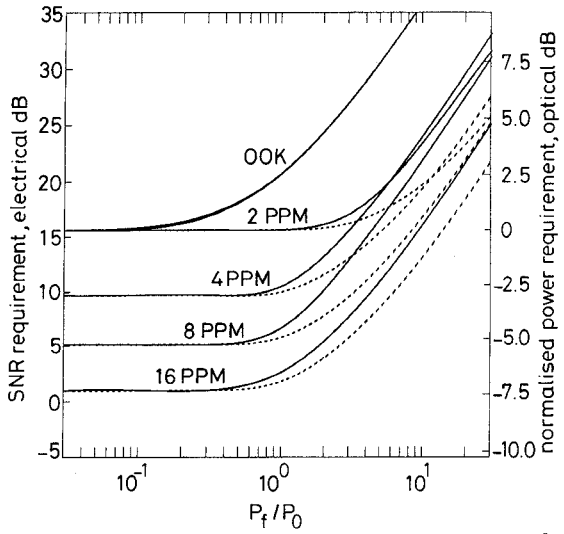

Fig. 7 *SNR and normalised optical power required to achieve 10^{-9} BER at 10Mbit/s against P_f/P_0 with no highpass filter for 22 and 45kHz lamps*
P_f maximum absolute excursion (with respect to the mean) of the received fluorescent optical power waveform
P_0 average optical power required to achieve 10^{-9} BER with OOK, in the absence of fluorescent lighting
On the right axis, 0dB corresponds to power P_0
——— 22kHz ballast
- - - - 45kHz ballast

We see in Fig. 7 that the SNR requirements for OOK are virtually identical with the 22 and 45kHz lamps. This is to be expected at the low BER being considered (10^{-9}) because, for a given ratio P_f/P_0, the worst-case values of the fluorescent-light samples are nearly the same. By contrast, for any order of PPM, at a given value of P_f/P_0, the SNR requirements with the 22kHz lamp are higher than those with the 45kHz lamp, since the 22kHz waveform has a larger maximum slope than the 45kHz waveform. If, instead, we compared the two lamps at the same mean received fluorescent-induced photocurrent (corresponding to the same useful lighting level), then we would use values of P_f/P_0 that are $1.125/0.582 \simeq 1.93$ times higher for the 45kHz lamp than for the 22kHz lamp (see Table 1), which would tend to equalise the impact of the two lamps. In all that follows, we consider the 22kHz lamp only.

Owing to the lowpass characteristic of the fluorescent-light interference, we would like to use a highpass filter to attenuate it, but this will induce ISI, thus incurring a power penalty. We will first quantify these ISI penalties in the absence of fluorescent lighting. Fig. 8 shows the electrical SNR penalties and optical power penalties induced in OOK and L-PPM links by the use of a first-order highpass filter, as a function of the filter 3dB cut-on frequency divided by the bit rate. The penalties in Fig. 8 were computed using the BER expressions given in Section 3.2, iteratively changing the SNR until the target BER of 10^{-9} was achieved. It is evident that L-PPM is much more tolerant of highpass filtering than is OOK, at least in the absence of line coding [11] or active baseline restoration [10, 11]. This is to be expected because the continuous PSD of the L-PPM signal goes to zero at DC, unlike that of OOK [2].

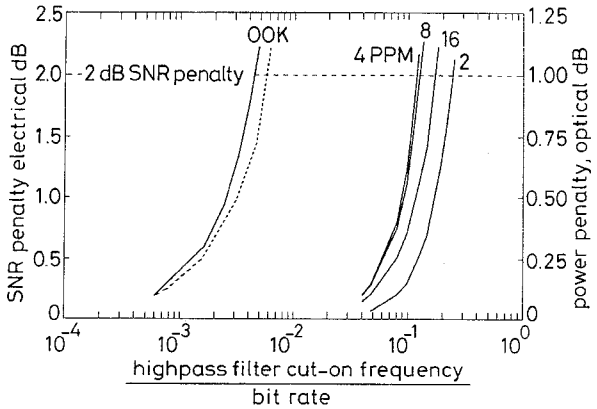

Fig. 8 *Electrical SNR penalty due to first-order highpass filtering in absence of fluorescent lighting at 10^{-9} BER*
——— exact method
– – – – Gaussian approximation

Considering OOK, when the highpass filter cut-on frequency is small compared to the bit rate, the filter impulse response spans many bit periods. Accordingly, the ISI introduced by highpass filtering is comprised of the weighted sum of many IID binary random variables. Therefore, the ISI can be approximated as a Gaussian noise [8] whose variance is proportional to the electrical signal power, and which can be computed using the known PSD of the modulated signal and the frequency response of the highpass filter. As shown in Fig. 8, approximating the ISI as Gaussian-distributed yields results in close agreement with those calculated using the exact enumeration method of Section 3.2. In the case of PPM, approximation of the ISI as Gaussian is less valid than for OOK, because the cut-on frequencies considered are not so small compared to the bit rate, and because the chip sequence is not IID.

When both fluorescent interference and highpass filtering are present, we would like to calculate the BER using the expressions given in Section 3.3, but the required computation is very intensive. Since we are only interested in computing SNR penalties here, we make some approximations as follows. Using the method in Section 3.1, we first calculate the SNR penalty caused by the fluorescent-light interference that has been filtered by the highpass filter. Next, in the absence of fluorescent lighting, we use the procedure in Section 3.2 to compute the SNR penalty caused by ISI from highpass filtering. We then approximate the total penalty as the sum of the fluorescent-light and ISI penalties that were calculated separately, an approximation that would be exact if the ISI were truly Gaussian-distributed. It is worth emphasising that although we exploit the approximate Gaussianity of the ISI to simply add the two penalties, we use ISI penalties calculated according to the exact enumeration method of Section 3.2.

In Figs. 9, 10 and 11, we present the SNR and power requirements of 1, 10, and 100Mbit/s links using various modulation schemes, and subject to 22kHz fluorescent interference. The requirements of OOK and PPM links without highpass filtering are computed in the same fashion as those in Fig. 7, using the BER expressions of Section 3.1. The requirements of links using first-order highpass filtering are calculated using the approximation described in the previous paragraph. Making use of the results of Fig. 8, we choose the highpass filter cut-on frequency so that the resulting ISI induces a 2dB SNR penalty (1dB optical power penalty) in the absence of fluorescent lighting. This choice, while somewhat arbitrary, represents a reasonable estimate of the highest cut-on frequency that could be used in the absence of line coding [11] or active baseline restoration [10, 11], in view of the steep rise of the penalties in Fig. 8. We note that our procedure results in a different choice of cut-on frequency for each modulation scheme and bit rate. Figs. 9, 10 and 11 also present the SNR and power requirements for a single BPSK subcarrier. In the absence of fluorescent lighting and multipath distortion, this modulation is known to require a 3dB higher SNR (1.5dB higher optical power) than OOK to achieve a given BER [2]. Since the subcarrier frequency can be chosen to lie well above the approximate 1MHz cutoff of the fluorescent interference, in principle, BPSK is virtually unaffected by this interference.

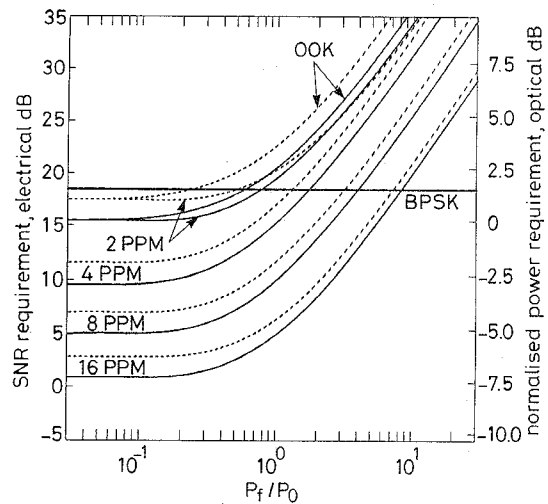

Fig. 9 *SNR and normalised optical power requirements for 10^{-9} BER against P_f/P_0 for 22 lamp with no highpass filter and with a highpass filter inducing a 2.0dB SNR penalty*
P_f maximum absolute excursion (with respect to the mean) of the received fluorescent optical power waveform
P_0 at each bit rate as the average optical power required to achieve 10^{-9} BER with OOK, in the absence of fluorescent lighting
On the right axis, 0dB corresponds to power P_0
The requirements for a BPSK subcarrier are also shown
Bit rate considered: 1Mbit/s
——— no highpass filter
– – – – 2.0 dB highpass filter

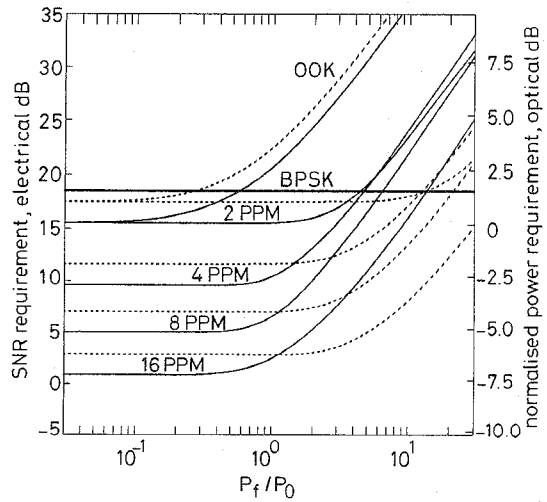

Fig. 10 *SNR and normalised optical power requirements for 10^{-9} BER against P_f/P_0 for 22 lamp with no highpass filter and with a highpass filter inducing a 2.0dB SNR penalty*
P_f maximum absolute excursion (with respect to the mean) of the received fluorescent optical power waveform
P_0 at each bit rate as the average optical power required to achieve 10^{-9} BER with OOK, in the absence of fluorescent lighting
On the right axis, 0dB corresponds to power P_0
The requirements for a BPSK subcarrier are also shown
Bit rate considered: 10Mbit/s
——— no highpass filter
– – – – 2.0 dB highpass filter

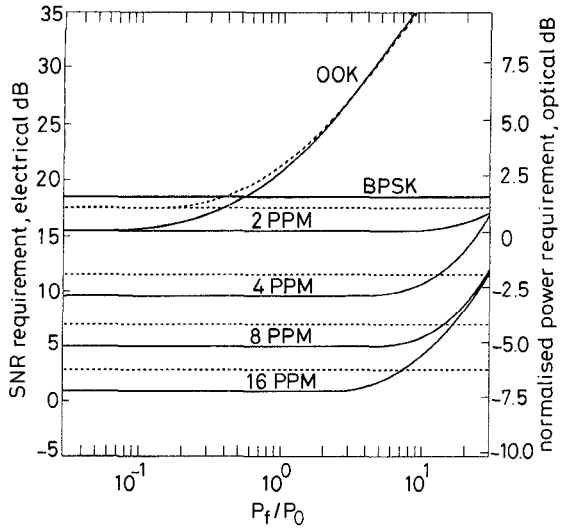

Fig. 11 *SNR and normalised optical power requirements for 10^{-9} BER against P_f/P_0 for 22 lamp with no highpass filter and with a highpass filter inducing a 2.0dB SNR penalty*
P_f maximum absolute excursion (with respect to the mean) of the received fluorescent optical power waveform
P_0 at each bit rate as the average optical power required to achieve 10^{-9} BER with OOK, in the absence of fluorescent lighting
On the right axis, 0dB corresponds to power P_0
The requirements for a BPSK subcarrier are also shown
Bit rate considered: 100Mbit/s
——— no highpass filter
– – – – 2.0 dB highpass filter

5 Discussion

Examining Figs. 9, 10 and 11, we see that among all modulation schemes considered, OOK is most susceptible to fluorescent-light interference, since the simple slicer is affected by the actual value of the fluorescent-light sample, in contrast to the PPM detector, which is sensitive only to differences among L successive samples. Without highpass filtering, the degradation of OOK is virtually the same at 1, 10 and 100Mbit/s, just as it was the same with the 22 and 45kHz lamps (see Fig. 7). As stated previously, this occurs at the low BER being considered (10^{-9}) because, for a given ratio P_f/P_0, the worst-case values of the fluorescent-light samples are nearly independent of bit rate and lamp frequency. Figs. 9, 10 and 11 show that, at all three bit rates, highpass filtering is not effective in improving the performance of OOK, because only very low cut-on frequencies (about $0.005R_b$) are permissible. The use of line coding can permit an increase in the filter cut-on, at the expense of reduced throughput; e.g. a rate-7/8 polarity-pulse code would permit a cut-on frequency of $\sim 0.03R_b$ [11]. Active baseline restoration can enable the use of a higher cut-on without loss of throughput; e.g. a cut-on frequency of $0.02R_b$ was achieved in [10] with little resulting ISI penalty. It is also possible that a higher-order highpass filter may prove more useful than a first-order filter.

The SNR penalties incurred by the L-PPM schemes decrease with increasing bit rate and also depend, to a lesser degree, on the order L. This is because the penalty depends upon the maximum difference between fluorescent-light samples within a given symbol period. At 1Mbit/s, all PPM orders incur penalties comparable to those for OOK, while at 10 and 100Mbit/s, the PPM penalties become progressively much smaller. At each bit rate, the penalty for 2 PPM is the smallest among the various PPM orders, since 2 PPM has the shortest symbol duration. Highpass filtering is more effective for L-PPM than for OOK. When the bit rate is 1Mbit/s, it is best not to use any highpass filter. At 10Mbit/s, the highpass filter inducing a 2dB ISI penalty provides a penalty reduction at large values of the ratio P_f/P_0. Given a choice of P_f/P_0, it would be possible to choose the filter cut-on frequency so as to minimise the overall performance penalty.

The choice of modulation scheme that leads to the minimum SNR (and optical power) requirement depends on the ratio P_f/P_0 and on the bit rate. We note that in directed links, P_f/P_0 can usually be made very small, while in non-directed links, P_f/P_0 can be as high as 1 to 10 [10]. At 1Mbit/s, 16 PPM without highpass filtering is the best choice, except for the largest values of P_f/P_0, where BPSK is superior. For 10Mbit/s, 16 PPM is the best scheme, and it may prove beneficial to use an optimised highpass filter. At 100Mbit/s, 16 PPM is again the best choice, and use of an optimised highpass filter will yield some improvement at the highest values of P_f/P_0.

Finally, we note that this study has considered only the time-averaged BER, and has only considered measures at the lowest system level (channel modulation and demodulation) for achieving this BER. If the system is indeed designed to achieve an average BER of 10^{-9}, then little can be done to exploit the burstiness of errors. On the other hand, an alternative system design strategy is to design the modulation/demodulation to achieve a somewhat higher average BER, and to reduce this to the required value through error-correction coding, possibly in conjunction with interleaving. For example, considering OOK at 1Mbit/s in the presence of 22kHz lighting, the system might be designed so within each group of 45bits, a few channel errors occur. In this case, an error-correction code with a block length several times longer than 45bits, and capable of correcting the requisite number of errors, could be used. Considering the same situation at a bit rate of 100Mbit/s, within each group of 4500 bits, a few bursts of ~100 channel errors would occur. In this case, candidate strategies would include: (i) using interleaving over an interval longer than 4500 bits, coupled with an error-correction code capable of correcting errors at the resulting time-averaged BER, or (ii) transmitting packets of duration shorter than ~1000 bits, retransmitting packets that are lost due to channel errors.

6 Conclusions

Using measured emissions from fluorescent lamps driven by electronic ballasts, we have evaluated the performance of OOK and L-PPM infrared links in the presence of this interference. Among the modulation techniques investigated, L-PPM is less susceptible than OOK to degradation from fluorescent lighting, particularly at higher bit rates. We have shown that in the absence of line coding or active baseline restoration, a first-order highpass filter is not effective in mitigating the impairment of OOK systems. Such a filter is useful in improving the performance of L-PPM schemes, particularly at high bit rates and when the fluorescent-light signal is strong. Under almost all of the conditions we considered, 16 PPM yields the highest average-power efficiency among all the schemes evaluated.

7 Acknowledgments

This work has been supported by National Science Foundation Grant Number ECS-9408957, the Hewlett-Packard Company, and the University of California MICRO Program. We thank C.S. Lee and G.W. Marsh for fluorescent light measurements and helpful discussions. We are grateful to W. Lapatovich of GTE Sylvania Laboratories for the data in Fig. 1.

7 References

1 GFELLER, F.R., and BAPST, U.H.: 'Wireless in-house data communication via diffuse infrared radiation', *Proc. IEEE*, 1979, **67**, pp. 1474–1486
2 BARRY, J.R.: 'Wireless infrared coomunication' (Kluwer Academic Press, Boston, 1994)
3 KAHN, J.M., BARRY, J.R., AUDEH, M.D., CARRUTHERS, J.B., KRAUSE, W.J., and MARSH, G.W.: 'Non-directed infrared links for high-capacity wireless LANs', *IEEE Pers. Commun.*, 1994, **1**, (2), pp. 12–25
4 KAHN, J.M., KRAUSE, W.J., and CARRUTHERS, J.B.: 'Experimental characterization of non-directed indoor infrared channels', *IEEE Trans. Commun.*, 1995, **43**, (4), pp. 1613–1623
5 KOTZIN, M.D.: 'Short-range communications using diffusely scattered infrared radiation'. PhD dissertation, Northwestern University, June 1981
6 MOREIRA, A.J.C., VALADAS, R.T., and DE OLIVEIRA DUARTE, A.M.: 'Characterization and modeling of artificial light interference in optical wireless communication systems'. Proceedings of 6th IEEE symposium on *Personal, indoor and mobile radio communications*, Toronto, Canada, 27–29 September 1995
7 MOREIRA, A.J.C., TAVARES, A.M.R., VALADAS, R.T., and DE OLIVEIRA DUARTE, A.M.: 'Modulation methods for wireless infrared transmission systems: performance under ambient light noise and interference'. SPIE Proc. on *Wireless data transmission*, Philadelphia, PA, USA, 23–25 October 1995, Vol. 2601, pp. 226–237
8 BARRY, J.R., KAHN, J.M., KRAUSE, W.J., LEE, E.A., and MESSERSCHMITT, D.G.: 'Simulation of multipath impulse response for wireless optical channels', *IEEE J. Sel. Areas in Commun.*, 1993, **11**, (3), pp. 367–379
9 AUDEH, M.D., KAHN, J.M., and BARRY, J.R.: 'Performance of pulse-position modulation on measured non-directed indoor infrared channels', *IEEE Trans. Commun.*, 1996, **4**, (6), pp. 654–659
10 MARSH, G.W., and KAHN, J.M.: '50 Mb/s infrared free-space link using on-off keying with decision-feedback equalization', *IEEE Photonics Technol. Lett.*, 1994, **6**, pp. 1268–1270
11 AUDEH, M.D., and KAHN, J.M.: 'Performance evaluation of baseband OOK for wireless indoor infrared LANs operating at 100 Mb/s', *IEEE Trans. Commun.*, 1995, **43**, (6), pp. 2085–2094